第36卷第1期
2017年2月

红外与毫米波学报
J. Infrared Millim. Waves

Vol. 36, No. 1
February, 2017

文章编号: 1001 - 9014(2017)01 - 0020 - 05

DOI:10.11972/j.issn.1001 - 9014.2017.01.005

Threshold power of 1.2 μm infrared laser by in-band pumped Ho^{3+} -doped crystal

CHEN Xiu-Yan[1,2*], ZHANG Pei-Xiong[1], JIANG Hua-Wei[1], HANG Yin[1], FENG Yan[1*]

(1. Shanghai Key Laboratory of Solid State Laser and Application, Shanghai Institute of Optics and Fine Mechanics, Chinese Academy of Sciences, Shanghai 201800, China;
2. College of Physics Science and Technology, Shenyang Normal University, Shenyang 110034, China)

Abstract: The threshold power of 1.2 μm laser generated from the Ho^{3+}:LLF crystal was discussed. Two typical quasi-three-level theoretical models were used to analyze the effectiveness of 1194 nm laser's threshold power in the in-band pumping source of 1.15 μm fiber laser with different parameters, such as the absorption coefficient of laser medium, the laser beam radius, the crystal length and reflectivity of the output mirror. It was found that the re-absorption loss was the most important factor leading to the different results for the two models, and the second model was close to the practice because of the narrow bandwidth pumping beam(<6 nm). The results provided reliable data of Ho^{3+}-doped 1.2 μm solid-state laser systems for the design and experimental research in further.

Key words: 1.2 μm infrared laser, in-band pumped, Ho^{3+}-doped crystal, threshold power
PACS: 8.20.-e, 78.20.Bh, 42.55.Ah, 42.60.By

同带泵浦 Ho^{3+} 激光晶体 1.2 μm 波段红外激光阈值功率

陈秀艳[1,2*], 张沛雄[1], 姜华卫[1], 杭 寅[1], 冯 衍[1*]

(1. 中国科学院上海光学精密机械研究所 空间激光信息技术研究中心, 上海 201800;
2. 沈阳师范大学 物理科学与技术学院, 辽宁 沈阳 110034)

摘要: 为探索同带泵浦掺杂 Ho^{3+} 激光晶体 1.2 μm 波段红外激光输出,采用掺杂浓度为 1 at% 的 Ho^{3+}:LLF 激光晶体作为激光增益介质,应用两种典型准三能级理论模型,计算了 Ho^{3+} 在 $^5I_6$ 和 $^5I_8$ 能级间跃迁辐射 1.19 μm 激光的阈值功率,分析了泵浦光和激光束腰半径、激光晶体长度、吸收损耗、腔镜反射率等参量与阈值功率的变化关系,得出了吸收损耗是影响阈值功率最敏感因素的重要结论,确定了泵浦阈值功率的范围,为后续 1.2 μm 波段红外激光实验研究提供了可靠的理论参考数据.

关 键 词: 1.2 μm 红外激光; 同带泵浦; Ho^{3+} 激光晶体; 阈值功率

中图分类号: O432.1 + 2 **文献标识码**: A

Introduction

With the development of optical mediums and laser technologies, many new lasers have been investigated and applied in various fields[1]. The beams, which possess the spectral region from 1.1 μm to 1.2 μm, have attracted much attention because of the pumping sources and the fundamental lights of yellow beams [2]. In recent years, many studies have reported that 1.1 ~ 1.2 μm coherent lights can pump Tm^{3+}-Ho^{3+}-co-doped fiber lasers[3], and many frequency doubled lasers (576 nm, 577 nm, 589 nm, 592 nm) were applied in the domain of astronomy, bio-medicine, cosmetology, high resolution spectroscopy[4]. Generally speaking, 1.2 μm lasers can be generated from Yb^{3+}-doped fiber lasers, Raman solid-state lasers, diode lasers, He-Ne gas lasers[5], and so on. As we known, Ho^{3+}-doped gain mediums are fa-

Received date: 2016-06-12, **revised date**: 2016-08-05 **收稿日期**:2016-06-12, **修回日期**:2016-08-05
Foundation items: Supported by National High-tech R & D Program of China (863 Program) (2015XXXXX), National Natural Science Foundation of China (61603265), Project of Shenyang Normal University (L201522), Training Programs for College Students' Innovation and Entrepreneurship (2016306-14171030)
Biography: Chen Xiuyan (1978-), female, Shanghai, Post-doctoral. Research area involves novel lasers, optical images.
* **Corresponding author**: E-mail: haomisschen@163.com; feng@siom.ac.cn

mous for working on 2 μm[6]. In fact, they are also promising candidates for 1.2 μm coherent sources because Ho^{3+} ions can emit plenty of spectral lines in the range from visible to infrared. Recently, Arizona University reported a series of CW and Q-switched 1.2 μm lasers generated from the Ho^{3+}-ZBLAN fibers. For example, Zhu et al. firstly reported a 1200 nm single-frequency laser from the Ho^{3+}-ZBLAN fiber in 2012[7] and the 1200 nm laser's power had been increased to Watt-level in 2014[8]. In 2015, a 0.44 μJ - 5.7 μs - 1190 nm laser was generated by means of a grapheme Q-switched short-length holmium-doped ZBLAN fiber[9]. However, there are few reports on the 1.2 μm holmium-doped solid-state laser system. Among many rare earth ions doped crystals, Ho^{3+}-doped fluoride crystals are of good characteristics of the low phone energy and thermal lens effects, which is similar to the Ho^{3+}-ZBLAN fibers. In this work, a 1 at% Ho^{3+}:LLF crystal was firstly chosen as an example for emitting the 1.19 μm laser, and a 1.15 μm fiber laser served as the pumping source. According to the quasi-three levels theory[10], two typical theoretical models were adopted to analyze the threshold power with different parameters. The results demonstrated that the crystal's re-absorption loss is the most important parameter influencing on the threshold power, and all of the theoretical results can be beneficial to further experiment research in future.

1　Calculation with Two Models

As shown in Fig. 1, the 1.2 μm fluorescence spectrum can be generated by Ho^{3+} ions transmitting from the energy level $^5I_6$ to $^5I_8$, which belongs to a quasi-three level system. Compared with the four level systems, many activation ions always stay in the low laser level $^5I_8$ in this system. In addition, the serious re-absorption loss can further result in the high threshold pumping power and the low efficiency. Therefore, it is quite necessary to analyze the influence of the re-absorption loss on the pumping threshold power.

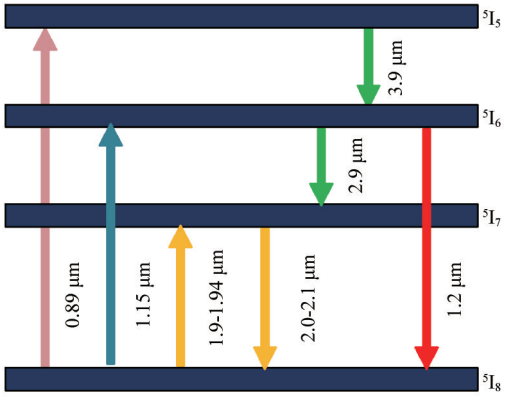

Fig. 1　Partial energy level of Ho^{3+} – doped crystal
图 1　掺杂 Ho^{3+} 离子晶体部分能级图

The first typical quasi-three-level equations were described as follows[11].

$$dN_2(r,z)/dt = f_2 Rr_p(r,z)-[N_2(r,z)-N_2^0]/\tau - \{f_2 c\sigma[N_2(r,z)-N_1(r,z)]/n\}\phi\varphi_0(r,z) \quad , \quad (1)$$

$$dN_1(r,z)/dt = -f_1 Rr_p(r,z)-[N_1(r,z)-N_1^0]/\tau + \{f_1 c\sigma[N_2(r,z)-N_1(r,z)]/n\}\phi\varphi_0(r,z) \quad , \quad (2)$$

$$d\phi/dt = (c\sigma/n)\iiint \Delta N(r,z)\ \phi\varphi_0(r,z)\,dV - \phi c(L+T)/(2nl) \quad , \quad (3)$$

where N_2 and N_1 are the actual population density in the upper and lower laser levels, respectively. N_1^0 and N_2^0 are the un-pumped population density. f_1 and f_2 are the Boltzmann constants for the laser lower and upper energy levels, respectively. σ is the emission cross section. τ is the lifetime of upper energy level. $L+T$ is the round-trip loss. l is the crystal length. σ is the photon density in the resonator. $r_p(r,z)$ and $\varphi_0(r,z)$ are normalized spatial distribution functions for the pumping light and the laser beam. n is the crystal's refractive index. $\Delta N(r,z)$ is the population inversion density.

$$\Delta N(r,z) = \{\tau(f_1+f_2)Rr_p(r,z)-N_1^0\}/[1+c\sigma\tau(f_1+f_2)\phi\varphi_0(r,z)/n] \quad . \quad (4)$$

By means of the equations above, the threshold power could be obtained.

$$P_{th} = [\pi h\nu_p(\omega_L^2+\omega_p^2)(L+T+2\sigma N_1^0 l)]/(4\sigma\tau\eta_a f) \quad , \quad (5)$$

$$f = f_1 + f_2 \quad , \quad (6)$$

where η_a is the absorption efficiency. h is the plank constant. ν_p is the frequency of pumping light. ω_l and ω_p are beam radius on the laser crystal for the coherent laser and the pumping light, respectively.

For the parameters above, N_1^0 is usually regarded as the total activation particles' density in some articles[20]. While in some other reports, it is the population density only in the low laser level. Here, it was considered as the former one so as to compare with the following calculation model.

Different from the first model, anther threshold power formula is shown in the following expressions[12].

$$P_{th} = [\pi h\nu_p(L/2+T/2+g_u f_1\sigma N_1^0 l/g_d)]/[2\sigma\tau\alpha\eta_p\eta_s(f_2+g_u f_1/g_d)F(L,\omega_l\,\omega_p)] \quad , \quad (7)$$

$$F(L,\omega_{(l,)}\,\omega_p) = \int_0^l \exp(-\alpha z)\,dz/[\omega_l^2(z)+\omega_p^2(z)] \quad , \quad (8)$$

where η_p is the quantum efficiency. $\omega_l(z)$ and $\omega_p(z)$ are the pumping light and coherent lasers' beam radius at z position. g_u is the laser upper level's energy degeneracy, and g_d is the laser lower level's energy degeneracy.

By comparing with the above two models, some differences could be found as follows: I) The energy degeneracy g_u and g_d were introduced into the re-absorption loss and the Boltzmann constants in the second model. II) The quantum efficiency η_p and the stokes shift efficiency appeared in the model two, where $\eta_p = 1$ and $\eta_s = \lambda_p/\lambda_s = 0.966$. The wavelengths of the pumping light and the coherent light were 1 152 nm and 1 194 nm, respectively. It can be seen that η_p and η_s hardly resulted in decisive disparity for the two models. III) The 1152 nm and 1194 nm beams' radii were not concrete values in the second model, and the optical field distribution in

the laser medium was considered[22], while the beams' radii were constants in the first model. IV) The most important factor was that the laser lower energy level's Boltzmann constant f_1 was introduced into the re-absorption loss in the second model, which greatly decreased the threshold power value, while N_1^0 is the total particle number density in the first model.

2 Discussion and Results

Both the two models were usually adopted in the quasi-three-level laser design. In order to discuss the re-absorption loss, we calculated the 1.2 μm laser's threshold power and analyzed the influencing factors by using the two models mentioned above. According to the Ho^{3+} absorption characteristics[17], the pumping laser's wavelength was determined by 1152 nm belonging to the same band with the 1194 nm coherent light, and the absorption efficiency was about 1. The pumping light and the laser beam were of the same wave radius. The parameters used for calculation were listed in Table 1. The Boltzmann constants for the laser lower and upper energy levels were obtained by the stark energies of $^5I_6$ and $^5I_8$.

After the calculations and simulations, the relationship of the absorption coefficient α and the threshold pumping power P_{th} were illustrated in Fig. 2a and Fig. 2b, respectively.

Figures 2(a-b) plotted the results of the mode one and mode two, respectively. They had the same changing law under the same condition. When the absorption coefficient exceeded 0.6 cm^{-1}, the P_{th} changed slowly. The smaller the beam radius is, the less the threshold power is. However, the values of the threshold powers are quite different for the two models. The reason can be explained as follows: for one thing, the Boltzmann constant f_1 was included in the model two, but not in model one. For another, the most important factor N_1^0 in the model one and model two had quite different physical meanings. If condition permitted, it is quite necessary to measure the re-absorption loss.

Moreover, the beam radius could be seriously affected by the P_{th} (Fig. 3). In the model one, the beam radius should be limited within 50 μm, while it could be expanded to several hundreds micrometers in the model two, which would reduce the power density and crystal's damage obviously.

Then the output coupler mirror's reflectivity R_2 with the P_{th} was simulated in Fig. 4. It could be found that the beam radius values were 50 μm and 20 μm, respectively, in the model one, while 150 μm and 50 μm in the model two. One can see that the threshold power in the model one is always larger than the model two when the wave radii are both 50 μm. In addition, the smaller the beam radius is, the higher the power intensity is, and the easier the laser crystal is damaged. Therefore, the

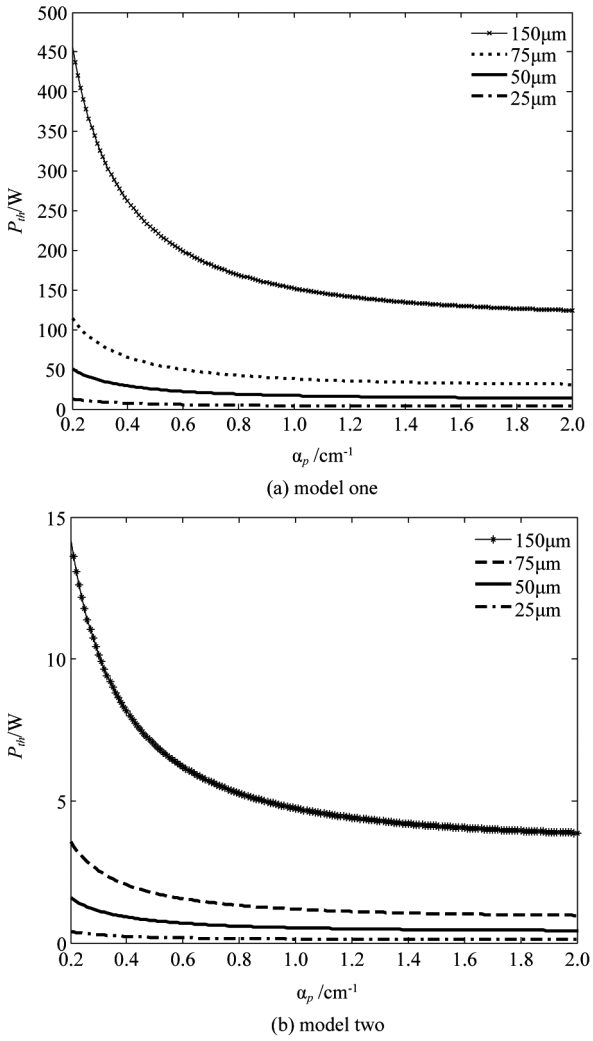

Fig. 2 The relationship of threshold power and absorption coefficient
图2 晶体吸收系数与阈值功率的关系(a)模型一(b)模型二

beam radius was set at about 150 μm in the model two. The threshold power P_{th} reduced quickly and is low with increasing of the output mirror's reflectivity R_2, even there appeared a critical point 76.5%, where the P_{th} values were equal in the two models.

The laser crystal's length in different models was discussed (Fig. 5). In each model, the optimum length was obtained, which corresponded to the smallest threshold pumping power, and the larger or smaller length could increase the P_{th} value. As a result, the best length in the model one was 2mm and in the model two was 11 mm.

According to the above discussion, it had a great gap between the two models, and the differences mainly resulted from the re-absorption loss. In the model one, the re-absorption loss is based on the populations in the

Table 1 Parameters for Calculation
表1 计算参数列表

parameters	h/ J·S	λ_p/μm	N/cm^{-3}	τ/ms	c/ m·s^{-1}	λ_l/μm	σ_e/cm^2	σ_a/cm^2	f_1	f_2
values	6.63×10^{-34}	1.15	1.58×10^{20}	1.8	3×10^8	1.19	0.85×10^{-20}	0.24×10^{-20}	0.028 8	0.112 2

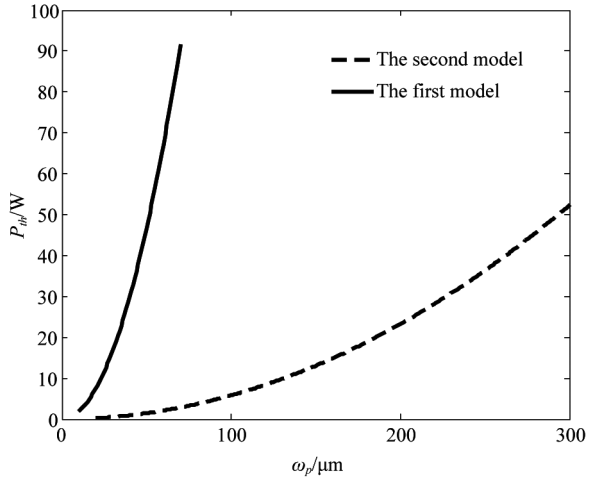

Fig. 3　The relationship of threshold power and beam radius
图 3　光斑半径与阈值功率关系图

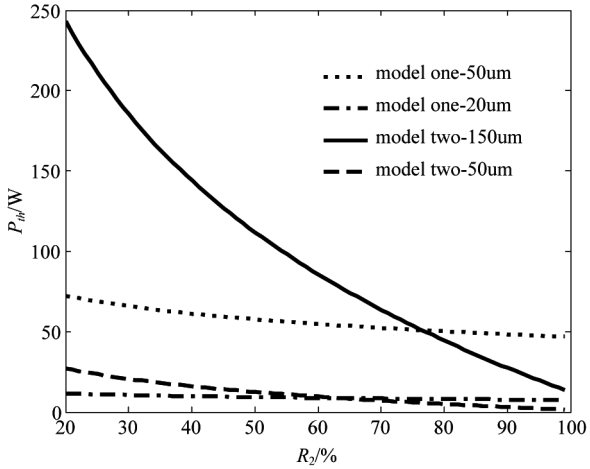

Fig. 4　The threshold power versus reflectivity
图 4　腔镜反射率与阈值功率关系图

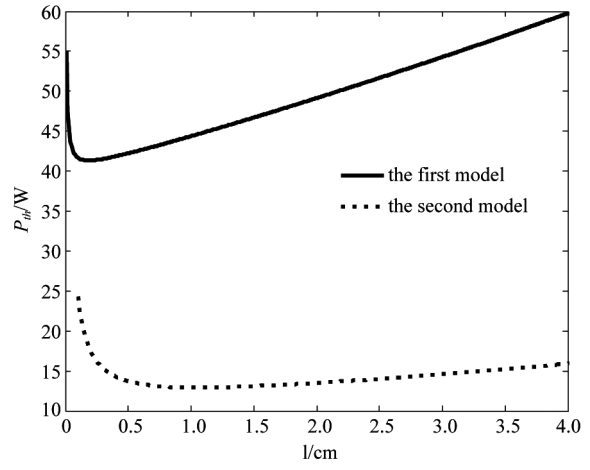

Fig. 5　The threshold power versus laser crystal length
图 5　激光晶体长度与阈值功率关系图

whole ground state level, but in the model two, the re-absorption loss aimed at the single-frequency laser emission. In fact, the experimental re-absorption loss and the threshold power may be between the two models' results. The reason is that there is spectral line width for both the pumping light and the coherent laser. Though the model two is more accurate than the model one owing to the energy degeneracy and Boltzmann constants, it is also based on the assumption that the pumping light and the coherent light are monochromatic. Therefore, both the two models offered the important data for laser design in different extent. According to the lab conditions, the spectrum line width of the 1152nm pumping light is less than 6nm, therefore, it is inferred that the model two is close to the experiment result. In addition, a problem worthy to be pointed out is that if the system parameters used are from the first model, they would also meet with the requirements of the model two.

3　Conclusions

In conclusion, two models were adopted for calculating the 1.2 μm light's threshold power under the in-band pumped Ho^{3+}: LLF quasi-three-level system. Though many differences existed between the two models, it provided the experimental research with important data.

References

[1] WANG Tao, LIU Gang, ZHOU Su-Hua, *et al*. A stable wavelength-spacing-tunable dual-wavelength single longitudinal mode fiber ring laser based on a DMD filter[J]. *Journal of Infrared and Millimeter Waves* (王涛, 刘刚, 周素华,等. 基于 DMD 滤波器的波长间隔可调谐的双波长单纵模光纤环形激光器. **红外与毫米波学报**), 2015, **34**(6):694 – 699.

[2] CHEN Xiu-Yan, LI Xiu, ZHANG Hao-Lei, *et al*. 589nm yellow laser generation by intra-cavity sum-frequency mixing in a T-shaped Nd: YAG laser cavity[J]. *Chinese Optics Letters*, 2009, **7**(9), 815 – 818.

[3] DONG Shu-Fu, CHENN Guo-Fu, ZHAO Shang-Hong, *et al*. Theoretical study on the 1180nm laser pumped Tm3 +, Ho3 + co-doped silica fiber laser[J]. *Laser Techology*, 2006, **30**(2):138 – 141.

[4] AUBERT C, VOS M H, MATHIS P, *et al*. FeIntraprotein radical transfer during photoactivation of DNA photolyase[J]. *Nature*, 2000, **405**(6786):586 – 590.

[5] SHNG S C, GERSTENBERGER D C. Advances in multiple wavelength He -Ne lasers, *Proceedings of SPIE*, 1987[C]., Los Angeles, CA: 1987, Lee R. Carlson, 76.

[6] SHEN Yin-Jie, YAO Bao-Quan, DUAN Xiao-Ming, *et al*. 103 W in-band dual-end-pumped Ho^{3+}:YAG laser[J]. *Optics Letters*, 2012, **37**(17):3588 – 3560.

[7] ZHU Xiu-Shan, ZONG Jie, Miller A, *et al*. Single-frequency Ho3 + -doped ZBLAN fiber laser at 1200 nm[J]. *Optics Letters*, 2012, **37**(20):4185 – 4187.

[8] ZHU Xiu-Shan, ZONG Jie, WIERSMA K, *et al*. Watt-level short-length holmium-doped ZBLAN fiber lasers at 1.2μm[J]. *Optics Letters*, 2014, **39**(6):1533 – 1536.

[9] LIU Shu-Jing, ZHU Xiu-Shan, ZHU Gong-Wen, *et al*. Graphene Q-switched Ho3 + -doped ZBLAN fiber laser at 1190 nm[J]. *Optics Letters*, 2015,**40**(2): 147 – 150.

[10] TAKUNORI T, TULLOCH W M, BYER R L. Modeling of quasi-three-level lasers and operation of cw Yb3 +:YAG lasers[J]. *Applied Optics*,1997, **36**(9): 1867 – 1874.

[11] RISK W P. Modeling of longitudinally pumped solid-state lasers exhibiting reabsorption losses[J]. *Journal of the Optical Society of America B*,1988, **5**(7):1412 – 1423.

[12] ZHU Jian, ZHANG Guang-Yin, CHEN Xiao-Bo. Theoretical analysis for Ho3 + laser threshold[J]. *Acta Physca Sinca* (朱箭,张光寅,陈晓波. Ho 激光器阂值的理论分析. **物理学报**), 1996, **45**(8): 1337 – 1343.